УДК 621.391

V.I. TIKHONOV
A.S. Popov Odessa national telecommunication academy

TENSOR MODEL OF I/Q-PHASE-MODULATED SIGNAL DETECTION

This paper studies theoretical issues of radio frequency multiplexing. A tensor model for I/Q-technique of phase modulation and demodulation of radiofrequency carrier introduced to provide flexible channel performance adaptation in OFDM radio access network due to the smooth variation of phase modulation depth in a wide range. The introduced method initiates advanced researches on physical layer of mobile and wireless networking based on implementation of piecewise linear functions in phase modulation of harmonic carrier signals. This method intends to contribute in future generation of mobile and wireless communication technologies.

Keywords: I/Q-modulation, OFDM, radio access, tensor model.

В.И. ТИХОНОВ
Одесская национальная академия связи им. А.С.Попова

ТЕНЗОРНАЯ МОДЕЛЬ ДЕТЕКТИРОВАНИЯ I/Q-ФАЗОВО-МОДУЛИРОВАННОГО СИГНАЛА

В статье рассматриваются теоретические вопросы радиочастотного мультиплексирования. Предложена тензорная модель I/Q-фазовой модуляции и демодуляции радиочастотной несущей для формализации принципа гибкой адаптации производительности канала в сети радиодоступа OFDM путем плавного изменением глубины фазовой модуляции в широком диапазоне. Описанный метод обосновывает новое направление исследований физического уровня мобильных и беспроводных сетей на основе применения кусочно-линейных функций для фазовой модуляции несущих гармонических сигналов. Данный метод направлен на разработку будущих поколений мобильных и беспроводных технологий связи.

Ключевые слова: I/Q-модуляция, OFDM, радиодоступ, тензорная модель.

1. Introduction

The method of in-phase/quadrature modulation (or I/Q-modulation) is widely used in wireless/mobile communications to form combined amplitude/phase modulated carrier signal which is utilized for orthogonal frequency division multiplexing (OFDM) [1–3]. In particular, the physical layer of long term evolution (LTE) of mobile/wireless communication technology is adopted for three optional types of I/Q modulation which are available to manipulate amplitude and/or phase of subcarriers in OFDM-composed signal [4–5]:

1) QPSK (quadrature phase shift keying);
2) 16QAM (quadrature amplitude modulation with 16 states);
3) 64QAM (quadrature amplitude modulation with 64 states).

The constellation diagrams of these three I/Q-modulation types are presented in Fig.1. The in-phase and quadrature components of the diagram (denoted I and Q) correspond respectively to cosine and sine components of complex exponent according to Euler formula [7]:

$$\rho \cdot exp(i \cdot \varphi) = \rho \cdot \left[cos(\varphi) + i \cdot sin(\varphi) \right]. \quad (1)$$

Consider the following relations to perform QPSK-signal (Fig.1-a) by $\rho = const$

$$\begin{cases} I = \rho \cdot cos(\varphi) \\ Q = \rho \cdot sin(\varphi) \end{cases}. \quad (2)$$

$$\rho \cdot exp(i \cdot \varphi) = I + i \cdot Q. \quad (3)$$

$$\varphi = \pm\left(\frac{\pi}{4} + n \cdot \frac{\pi}{2} \right) = \pm \frac{\pi}{4} \cdot (1 + 2 \cdot n), \quad n = 0,1,2,... \quad . \quad (4)$$

Therefore, QPSK provides I/Q-balanced modulation, e.g. $|I| \equiv |Q|$. The four states of QPSK constellation diagram in Fig.1-a imply 2 bit information beard by any of QPSK subcarriers. The QPSK-diagram (Fig.1-a) partitions the whole phase circle $\Phi = 2 \cdot \pi$ into four quadrants related to state-points “00”, “01”, “10” and “11” (due to the phase φ rotate positive direction); $\varphi = 0$ means $I = \rho$, $Q = 0$.

The 16QAM modulation drops each of four phase diagram quadrants in Fig.1-a into four states through different discrete phases and amplitudes, (Fig.1-b). The total number of states is 16, and information capacity of one subcarrier is 4 bits. Similarly, 64QAM (Fig.1-c) provides 6 bit for one sub-harmonic bearer. It is obvious, that QPSK modulation has maximal character spacing among three modulation types shown in Fig.1 and therefore, it is the most noise resistant technique; instead, this type provides minimal data transmission speed, e.g. minimal channel performance. No one of three given modulation types can be taken default as the best choice since conventional radio channel with multiple access requires limitation of critical bit error rate; the latter is dynamically changing along with the fluctuation of radio channel interconnection state.

The OFDM-composed LTE radio signal is performed with Δf =15 KHz frequency spacing, e.g. the first harmonic subcarrier is 15 KHz towards the central carrier signal f_0, Fig.2; this frequency determines the minimal

possible sampling time $T_{min} = \frac{1}{f_1} = 0.067ms$ for OFDM coding and decoding. The LTE 15 KHz frequency spacing is constant option for any of three types of I/Q-modulation adopted for LTE; thus, the total number of subcarriers depends on the dedicated frequency bandwidth.

Let any OFDM LTE subcarrier bears to be considered as one OFDM-*symbol* (of either 2, 4 or 6 bit depending of the dedicated type of modulation QPSK, 16QAM or 64 QAM respectively). Denote the full collection of all the OFDM symbols as one OFDM-*word*. Consider solely one side-band modulation applied in LTE PHY layer along with the $2 \times 0.25 = 0.5$ MHz guard band, the 5 MHz bandwidth of LTE utilizes 300 subcarriers: $(300 \times 15KHz) + 0.5MHz = 5MHz$. Respectively, the 20 MHz bandwidth of LTE utilizes 1200 subcarriers. The information capacity of one OFDM composition word for LTE 5MHz bandwidth is minimum $2bit \times 300 = 600bit$ for QPSK modulation and maximum $6bit \times 300 = 1800bit$ for 64QAM modulation.

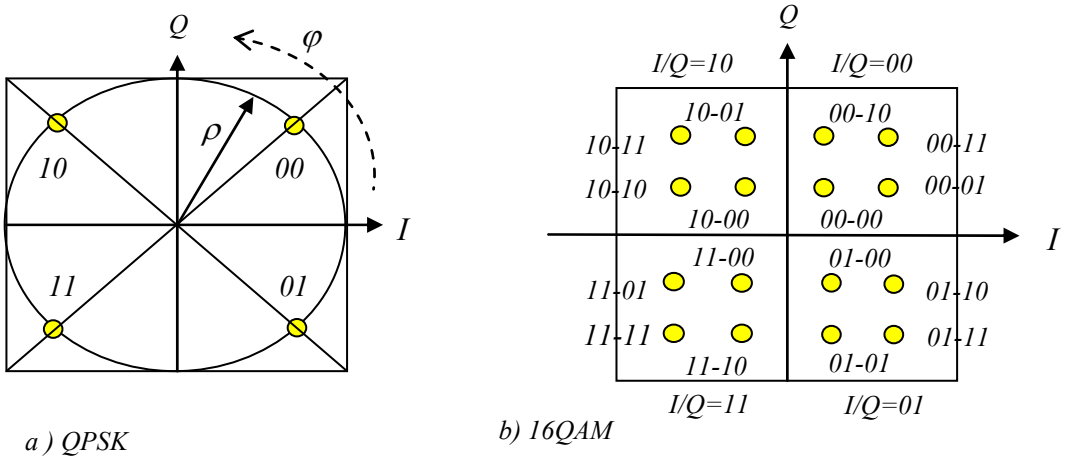

Figure 1 – Constellation diagrams for QPSK, 16QAM and 64QAM

The minimal and maximal information capacity of one OFDM composition word for LTE 20 MHz bandwidth is $2bit \times 1200 = 2400bit$ for QPSK modulation and $6bit \times 1200 = 7200bit$ for 64QAM modulation.

The instant bit rate and related spectral efficiency for any type of I/Q-modulation in LTE depends of the actual sampling time of OFDM-word. As mentioned above, the theoretic minimal sampling time T_{min} is determined by frequency spacing Δf. However, all of the three LTE adopted modulation types (QPSK, 16QAM and 64QAM) form the OFDM composed signals which are not continuous in time while going on from one OFDM-word to another one. For instance, the previous QPSK symbol is "00" and the next one is "11"; so, the phase function $\varphi(t)$ in word switching moment changes abruptly and the frequency $f(t) = \frac{\partial \varphi(t)}{\partial t} \to \infty$ tends to infinity at this very moment. To overcome this issue, the special recovering cyclic prefix (CP) is used in LTE framing [4].

There are two optional cyclic prefix lengths: normal and extended CP. If normal CP used, then word sampling time is $T_{norm} = \frac{0.5ms}{7} \approx 0.071ms$. If extended CP used, then $T_{ext} = \frac{0.5ms}{6} \approx 0.083ms$. So, the normal CP length is $\Delta T_{norm} = \frac{0.5ms}{7} - \frac{1}{15KHz} \approx \approx (0.071 - 0.067)ms = 0.004ms$; extended CP length is $\Delta T_{ext} = 0.083 - 0.067 \approx 0.016ms$.

The bit rate of LTE PHY layer for QPSK in 5 MHz bandwidth with normal CP is $R_{norm} = \frac{2bit \times 300}{0.071msec} = 8.4Mbps$; the bit rat with extended CP is $R_{ext} = \frac{2bit \times 300}{0.083msec} = 7.2Mbps$. The spectral efficiency of LTE PHY layer for QPSK is: $\gamma_{norm} = \frac{R}{\Delta F} = \frac{8.4Mbps}{5MHz} = 1.68bit$; $\gamma_{ext} = \frac{R}{\Delta F} = \frac{7.2Mbps}{5MHz} = 1.44bit$. These figures are collected in Tab.1.

It is clear that instant bit rate R of LTE PHY layer can be taken among six possible options for any given frequency bandwidth, i.e. for 5MHz bandwidth these are: $R \in$ (7.2; 8.4; 14.4; 16.8; 21.6; 25.2) Mbps.

Manipulating the PHY layer performance facilitates the LTE access adaptation to the current state of communication between the base station (BS) and user equipment (UE), e.g. to the radio interference issues. The more stable radio access is the higher channel bit rate can be chosen. However, some remarks are to be given herewith.

Firstly, solely six fixed options for channel bit rate are available; this limits the accuracy of channel performance adaptation.

Secondly, the LTE PHY layer operates with 10 millisecond frames, and each of them partially addresses to any of active user devices; so any one frame must be adjusted by BS to the fixed average bit rate acceptable to all the client's UEs; therefore, individual BS-to-UE adaptation is problematic.

Thirdly, the conventional orthogonal frequency division multiplexing method (OFDM) used in LTE PHY layer suffers known issue of enormous peak-to-average power ratio (PAR) which is character to combined phase and amplitude modulation; this phenomenon determines strict requirements to radio amplifier linearity in a wide power dynamic range.

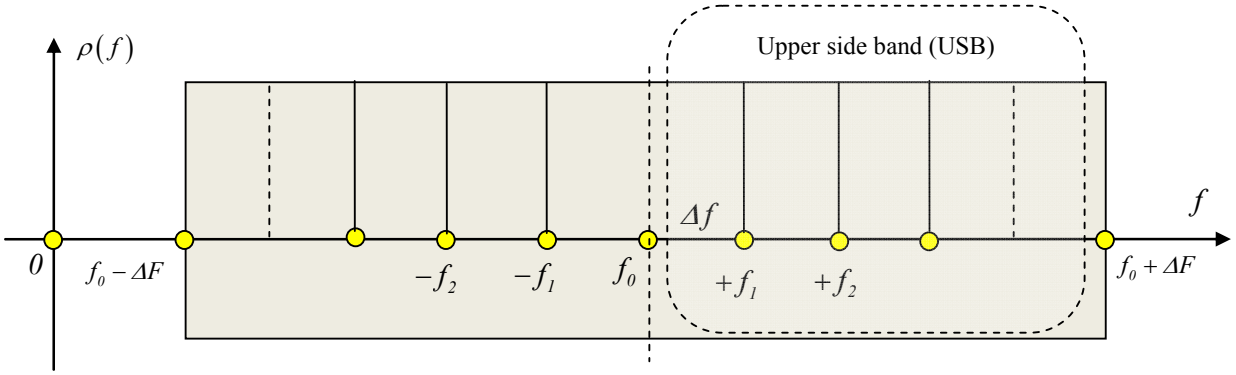

Figure 2 – OFDM subcarriers allocation in frequency bandwidth

Table 1 – Information capacity and spectral efficiency for LTE physical layer

Information capacity of the LTE OFDM word (bit/byte), Bit rate and spectral efficiency of the LTE PHY layer					Spectral efficiency $\gamma = \frac{R}{\Delta F}$ (bit)
Bandwidth ΔF (MHz)	5	10	15	20	
Information capacity QPSK (bit/byte)	600/75	1200/150	1800/225	2400/300	
Information capacity 16QAM (bit/byte)	1200/150	2400/300	3600/450	4800/600	
Information capacity 64QAM (bit/byte)	1800/225	3600/450	5400/675	7200/900	
Bit rate R (Mbps) for normal CP					$\gamma_{normCP} = 1.68$
QPSK	8.4	16.8	25.2	33.6	
16QAM	16.8	33.6	50.4	67.2	
64QAM	25.2	50.4	75.6	100.8	
Bit rate R (Mbps) for extended CP					$\gamma_{extCP} = 1.44$
QPSK	7.2	14.4	21.6	28.8	
16QAM	14.4	28.8	43.2	57.6	
64QAM	21.6	43.2	64.8	86.4	

The analysis leads to conclusion that more researches are needed with respect to the LTE inherent OFDM multiple access intended to more sophisticated adaptation of PHY layer radio channel performance. Based on this premise, *this work aims to substantiate theoretical background on flexible I/Q-based phase modulation of radiofrequency carrier to enhance channel performance adaptation in OFDM radio access network.*

2. Interference model of I/Q-modulation scheme

Commonly used theoretical model of combined phase and amplitude modulation is derived from the cosine harmonic function $\rho_t \cdot cos\left(\omega \cdot t + \varphi_t\right)$ presentation, where t is time, ω is angular frequency, ρ_t is amplitude modulation function and φ_t is phase modulation function; this presentation relies on the following trigonometry formula [7]:

$$cos\left(\alpha + \beta\right) = cos\,\alpha \cdot cos\,\beta - sin\,\alpha \cdot sin\,\beta\,, \tag{5}$$

$$\rho_t \cdot cos\left(\alpha + \beta\right) = \rho_t \cdot \left(cos\,\alpha \cdot cos\,\beta - sin\,\alpha \cdot sin\,\beta\right). \tag{6}$$

Substitute $\alpha = \omega \cdot t$ and $\beta = \varphi_t$ into the (6):

$$\rho_t \cdot cos\left(\omega \cdot t + \varphi_t\right) = cos\left(\omega \cdot t\right) \cdot \left(\rho_t \cdot cos\,\varphi_t\right) - sin\left(\omega \cdot t\right) \cdot \left(\rho_t \cdot sin\,\varphi_t\right). \tag{7}$$

Denote

$$\begin{cases} I_t = \rho_t \cdot cos\left(\varphi_t\right) \\ Q_t = \rho_t \cdot sin\left(\varphi_t\right) \end{cases}. \tag{8}$$

Considering (7) and (8) we obtain

$$\rho_t \cdot cos\left(\omega \cdot t + \varphi_t\right) = I_t \cdot cos\left(\omega \cdot t\right) - Q_t\, sin\left(\omega \cdot t\right). \tag{9}$$

The equation (9) is often taken as a math model of I/Q-modulation scheme, Fig. 3.

However, the given above reasoning of I/Q modulation scheme does not seem to be logically immaculate. In fact, an alternative model of the sine harmonic function $\rho_t \cdot sin\left(\omega \cdot t + \varphi_t\right)$ presentation can be offered [7]:

$$sin\left(\alpha + \beta\right) = sin\,\alpha \cdot cos\,\beta + cos\,\alpha \cdot sin\,\beta\,. \tag{10}$$

Based on (10) we obtain $\rho_t \cdot sin\left(\omega \cdot t + \varphi_t\right) = sin\left(\omega \cdot t\right) \cdot \left(\rho_t \cdot cos\,\varphi_t\right) + cos\left(\omega \cdot t\right) \cdot \left(\rho_t \cdot sin\,\varphi_t\right)$, or

$$\rho_t \cdot sin\left(\omega \cdot t + \varphi_t\right) = I_t \cdot sin\left(\omega \cdot t\right) + Q_t\, cos\left(\omega \cdot t\right). \tag{11}$$

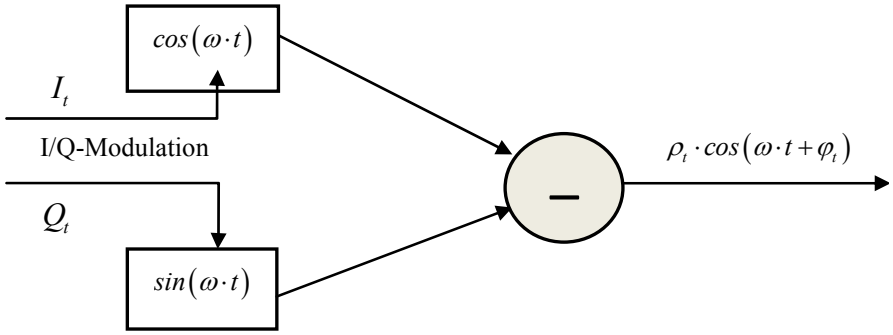

Figure 3 – Typical math model of I/Q-modulation scheme

The equation (11) leads to correspondent math model of I/Q-modulation scheme, Fig. 4. Two math models (9) and (11) along with two modulation schemes in Fig.3 and Fig.4 seem to be logically equivalent. The question arises – is the math model of (9) really preferable or not? To disambiguate the logical foundation of I/Q-modulation scheme we propose an alternative model of in-phase/quadrature modulation based on geometric tensor approach. Let transform the Euler formula (1) as following:

$$\rho_t \cdot exp\left[i \cdot \left(\omega \cdot t + \varphi_t\right)\right] = \rho_t \cdot exp\left(i \cdot \omega \cdot t\right) \cdot exp\left(i \cdot \varphi_t\right). \tag{12}$$

$$\begin{cases} exp\left(i \cdot \omega \cdot t\right) = cos\left(\omega \cdot t\right) + i \cdot sin\left(\omega \cdot t\right) \\ exp\left(i \cdot \varphi_t\right) = cos\,\varphi_t + i \cdot sin\,\varphi_t \end{cases}. \tag{13}$$

Following (9), (11) and (14) we obtain

$$\rho_t \cdot exp\left[i \cdot \left(\omega \cdot t + \varphi_t\right)\right] = \rho_t \cdot \left[cos\,\varphi_t \cdot cos\left(\omega \cdot t\right) - sin\,\varphi_t \cdot sin\left(\omega \cdot t\right) + i\left(cos\,\varphi_t \cdot sin\left(\omega \cdot t\right) + sin\,\varphi_t \cdot cos\left(\omega \cdot t\right)\right)\right],$$

or finally

$$\rho_t \cdot exp\left[i \cdot \left(\omega \cdot t + \varphi_t\right)\right] = I_t \cdot cos\left(\omega \cdot t\right) - Q_t \cdot sin\left(\omega \cdot t\right) + i\left(I_t \cdot sin\left(\omega \cdot t\right) + Q_t \cdot cos\left(\omega \cdot t\right)\right). \tag{14}$$

Comparing (12) and (13) we may conclude that complex presentation (14) integrates both cosine and sine based models of I/Q-modulation. According to tensor approach we simplify the integrated complex model (15) representing the I/Q-modulated signal in the special coordinate system with I^{ω} / Q^{ω} axis rotating along with I/Q axis. This representation is performed due to the multiplication by conjugate complex exponent $exp\left(-i \cdot \omega \cdot t\right)$:

$$\rho_t \cdot exp\left[i \cdot \left(\omega \cdot t + \varphi_t\right)\right] \rightarrow \rho_t \cdot exp\left[i \cdot \left(\omega \cdot t + \varphi_t\right)\right] \cdot exp\left(-i \cdot \omega \cdot t\right) = exp\left(i \cdot \varphi_t\right) = \rho_t \cdot \left[cos\left(\varphi_t\right) + i \cdot sin\left(\varphi_t\right)\right],$$

or

$$\rho_t \cdot exp\left[i \cdot \left(\omega \cdot t + \varphi_t\right)\right] \rightarrow I_t + i \cdot Q_t \tag{15}$$

The geometric presentation of (15) is a vector sum of two orthogonal vectors (denote $\vec{I}_t$ and $\vec{Q}_t$) rotating with the angular frequency $\omega = 2 \cdot \pi \cdot f$ calculated in *rad/sec* units

$$\vec{s}_t = \vec{I}_t + \vec{Q}_t, \tag{16}$$

where $f = \frac{1}{T}$ is rotating frequency calculated in *Hz*, T is rotating period in *second* units, Fig. 5.

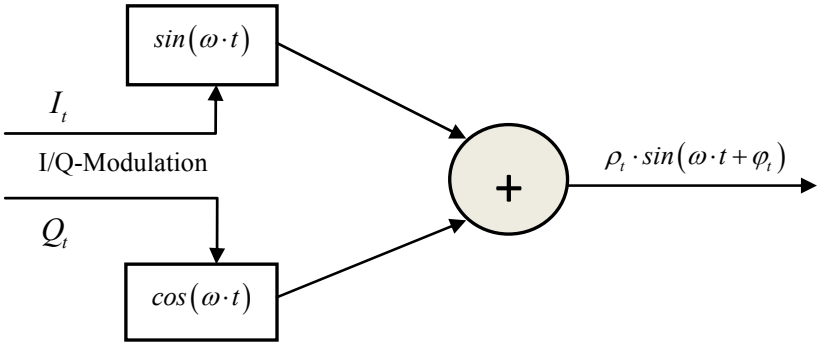

Figure 4 – Correspondent math model of I/Q-modulation scheme

The physical meaning of the vector sum (16) is interference of two coherent electromagnetic waves resulted in so called "standing wave" with the power magnitude $\left|\vec{s}_t\right|^2$ determined by the squared module of vector $\vec{s}_t$. The magnitude $\left|\vec{s}_t\right|^2$ is slowly changing in time t according to t modulation functions I_t and Q_t.

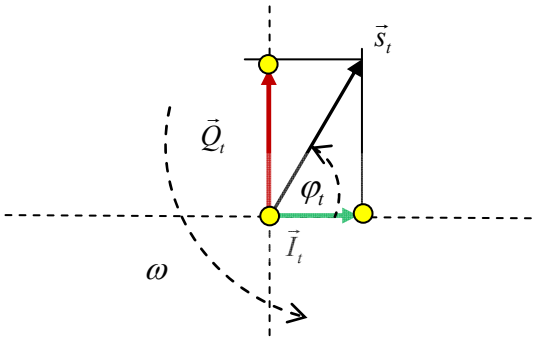

Figure 5 – Geometric presentation of I/Q-modulation scheme

Consider that $sin\left(\omega \cdot t\right) = cos\left(\omega \cdot t - \frac{\pi}{2}\right)$; therefore, according to geometric model (16) shown in Fig.5, the following functional model of I/Q-modulation scheme can be determined (Fig.6).

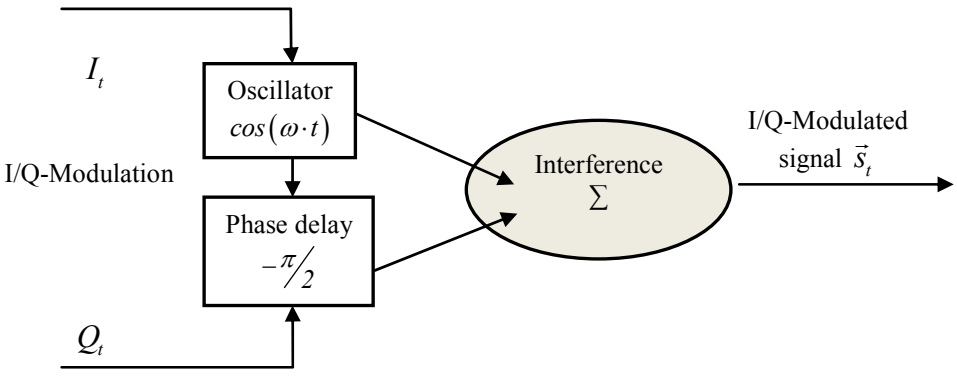

Figure 6 – Interference model of I/Q-modulation scheme

3. Tensor model of I/Q-demodulation process

The interference functional scheme of I/Q-modulation in Fig.6 predetermines the appropriate demodulation

algorithm applied at the receiving party of radio channel, Fig.7. Two values $\vec{D}_t^I$ and $\vec{D}_t^Q$ related to in-phase and quadrature components of receiving signal $\vec{s}_t$ are accepted by related I and Q detectors due to the interference of correspondent reference signals:

$$\begin{cases} \vec{D}_t^I = \vec{s}_t + \overrightarrow{cos}(\omega \cdot t) \\ \vec{D}_t^Q = \vec{s}_t + \overrightarrow{sin}(\omega \cdot t) = \vec{s}_t + \overrightarrow{cos}\left(\omega \cdot t - \frac{\pi}{2}\right) \end{cases}, \tag{17}$$

The geometric presentation of I/Q-demodulation process is presented in Fig.8. The complex system coordinate plane is created by two orthogonal axes: in-phase axis $\vec{x}$ and quadrature axis $\vec{y}$. To form the correspondent coordinate basis $(\vec{e}_x, \vec{e}_y)$ a special scheme of frequency and phase synchronization of local oscillator in Fig.7 is applied. Due to this synchronization, the local oscillator frequency is kept equal to the frequency of central carrier in receiving signal $\vec{s}_t$; again, the null-phase positioning can be achieved conventionally (e.g. if $|\vec{I}_t| = |\vec{Q}_t|$ in return to zero modulation moment).

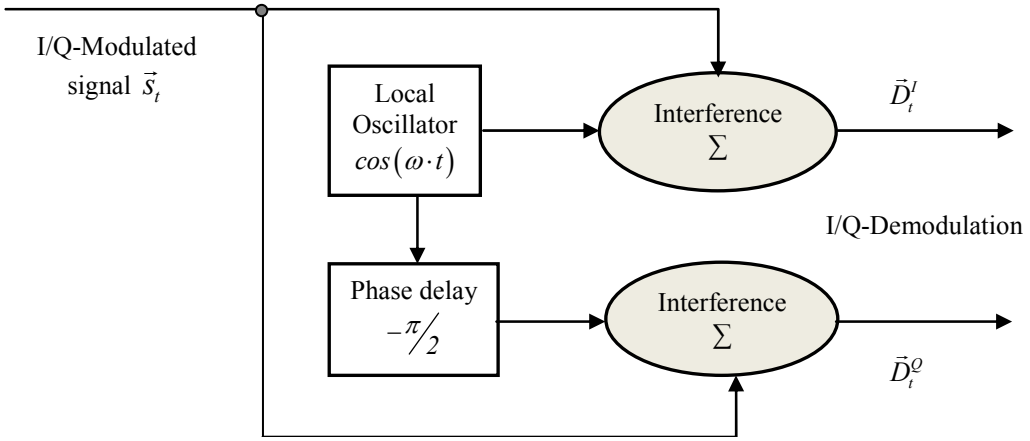

Figure 7 – Interference model of I/Q-demodulation scheme

According to the geometric presentation of signal interference in I-detector, we have

$$\begin{cases} \vec{D}_t^I = \vec{s}_t + \vec{e}_x \\ \vec{D}_t^Q = \vec{s}_t + \vec{e}_y \end{cases}, \tag{18}$$

where $\vec{e}_x$ and $\vec{e}_y$ are unitary vectors of $\vec{x}$ and $\vec{y}$ axes.

Let's present vector $\vec{D}_t^I$ in the new affine basis (denoted $\overrightarrow{Sx}$) created by two vectors: $\vec{s}_t$ and $\vec{e}_x$; this basis is neither orthogonal nor unitary. The metric tensor of $\overrightarrow{Sx}$ basis (denote $\underline{\underline{M}}_{SX}$) is formed by scalar product of vectors $\vec{s}_t$ and $\vec{e}_x$:

$$\underline{\underline{M}}_{SX} = \left\langle \overrightarrow{Sx} \times \overrightarrow{Sx} \right\rangle = \begin{bmatrix} \langle \vec{s}_t \times \vec{s}_t \rangle & \langle \vec{s}_t \times \vec{e}_x \rangle \\ \langle \vec{e}_x \times \vec{s}_t \rangle & \langle \vec{e}_x \times \vec{e}_x \rangle \end{bmatrix} = \begin{bmatrix} |\vec{s}_t|^2 & |\vec{s}_t| \cdot |e_x| \cdot cos\,\varphi_t \\ |\vec{s}_t| \cdot |e_x| \cdot cos\,\varphi_t & |e_x|^2 \end{bmatrix}. \tag{19}$$

Consider $|e_x| = 1$ after transformation we obtain

$$\underline{\underline{M}}_{SX} = \begin{bmatrix} |\vec{s}_t|^2 & |\vec{s}_t| \cdot cos\,\varphi_t \\ |\vec{s}_t| \cdot cos\,\varphi_t & 1 \end{bmatrix}. \tag{20}$$

In case $|\vec{s}_t| = |e_x| = 1$ (by using an appropriate amplifier factor) we get

$$\underline{\underline{M}}_{SX} = \begin{bmatrix} 1 & cos\,\varphi_t \\ cos\,\varphi_t & 1 \end{bmatrix}. \tag{21}$$

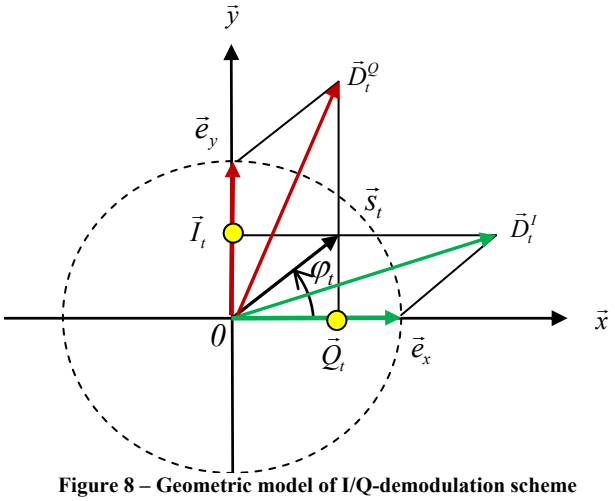

Figure 8 – Geometric model of I/Q-demodulation scheme

To obtain vector $\vec{D}_t^I$ module in coordinate system $\overrightarrow{Sx}$ apply known tensor analysis form [8]:

$$\left|\vec{v}\right|^2 = v^A \cdot \underline{\underline{A}} \cdot \left(v^A\right)^T, \tag{22}$$

where $\underline{\underline{A}}$ is metric tensor of linear system A created by the set of vectors emanated in the common zero-point; v^A is row-matrix of contravariant projection of vector $\vec{v}$ into the system A; $\left(v^A\right)^T$ is transposed row-matrix v^A (column-matrix). According the Fig.8 vector diagram, we have $\vec{v} = \vec{D}_t^I$, $v^A = [1,1]$; so

$$\left|\vec{D}_t^I\right|^2 = [1,1] \cdot \underline{\underline{M}}_{SX} \cdot [1,1]^T = [1,1] \cdot \begin{bmatrix} \left|\vec{s}_t\right|^2 & \left|\vec{s}_t\right| \cdot \cos\varphi_t \\ \left|\vec{s}_t\right| \cdot \cos\varphi_t & 1 \end{bmatrix} \cdot [1,1]^T. \tag{23}$$

After transformation the (23) we obtain the following:

$$\left|\vec{D}_t^I\right|^2 = \left|\vec{s}_t\right|^2 + 2 \cdot \left|\vec{s}_t\right| \cdot \cos\left(\varphi_t\right) + 1. \tag{24}$$

If signal $\vec{s}_t$ is normalized by the amplifier as $\left|\vec{s}_t\right| = 1$ then

$$\left|\vec{D}_t^I\right|^2 = 2 \cdot \left(1 + \cos\left(\varphi_t\right)\right). \tag{25}$$

Applying similar reasoning with respect to the quadrature component we get in general case

$$\left|\vec{D}_t^Q\right|^2 = \left|\vec{s}_t\right|^2 + 2 \cdot \left|\vec{s}_t\right| \cdot \sin\left(\varphi_t\right) + 1. \tag{26}$$

In particular case of $\left|\vec{s}_t\right| = 1$ the following relation is valid:

$$\left|\vec{D}_t^Q\right|^2 = 2 \cdot \left(1 + \sin\left(\varphi_t\right)\right). \tag{27}$$

Based on relationships (24) – (27) the data acquisition towards the phase-modulated signal

$$\vec{s}_t = exp\left[i \cdot \left(\omega \cdot t + \varphi_t\right)\right] = \cos\left(\omega \cdot t + \varphi_t\right) + i \cdot \sin\left(\omega \cdot t + \varphi_t\right) \tag{27}$$

can be achieved. To perform this data acquisition a comparison of two signals is needed (i.e. $\left|\vec{D}_t^I\right|^2$ and $\left|\vec{D}_t^Q\right|^2$).

4. Linear weighted phase detection of I/Q modulated signal

Reconstruction of phase function φ_t at the receiving party of the radio channel can be performed within the range of $\varphi_t \in (-\pi, +\pi)$ due to the joint account of two factors: in-phase and quadrature components of the phase detector (i.e. $\left|\vec{D}_t^I\right|^2$ and $\left|\vec{D}_t^Q\right|^2$). This reconstruction is based on the two functions of sine and cosine derived from (25) and (27):

$$\sin\varphi_t = \frac{\left|\vec{D}_t^Q\right|^2}{2} - 1; \cos\varphi_t = \frac{\left|\vec{D}_t^I\right|^2}{2} - 1. \tag{28}$$

The inverse functions of sine and cosine ($arcsin\,\varphi_t$ and $arccos\,\varphi_t$) are shown in Fig. 9 along with related functions $\cos\varphi_t = f_1\left(\sin\varphi_t\right)$ and $\sin\varphi_t = f_2\left(\cos\varphi_t\right)$, where index t in φ_t function is omitted for simplicity. It is clear that function $\varphi = arcsin\,\varphi$ is critically sensitive to the deviation of the $\sin\varphi$ argument in the edge neighborhoods of two points: $\sin\varphi = 1$ and $\sin\varphi = -1$ in Fig.9-a.

Therefore, because of that singularity, the reconstruction of the phase φ via the function $\varphi = arcsin\,\varphi$ is

not accurate within the said neighborhoods $|sin\varphi| \to 1$. At the same time one can see that function $cos\varphi = f_1(sin\varphi)$ tends to zero if $|sin\varphi| \to 1$. Likewise the $arcsin\varphi$ function, the inverse function $arccos\varphi$ in Fig.9-b is also singular towards neighborhoods $|cos\varphi| \to 1$, and therefore, function $sin\varphi = f_2(cos\varphi)$ tends to zero if $|cos\varphi| \to 1$.

Based on this reasoning, we introduce balanced linear weighted formula for reconstruction of the phase function φ_t at the receiving party of the radio channel with respect to the first quadrant of complex phase plane (index t in φ_t is omitted for simplicity):

$$\varphi = \frac{1}{cos\varphi + sin\varphi} \cdot (arcsin\varphi \cdot cos\varphi + arccos\varphi \cdot sin\varphi). \tag{29}$$

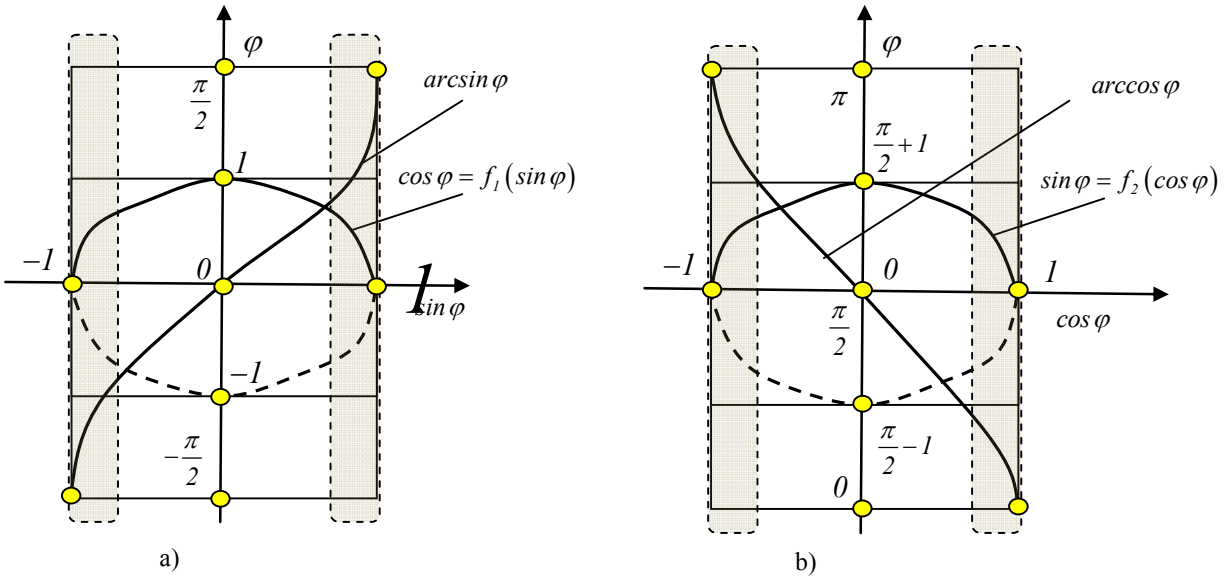

Figure 9 – Inverse functions of sine and cosine

It is obvious, that if no mistake occurs, then $arcsin\varphi = arccos\varphi = \varphi$ and relationship (29) turns into the identity $\varphi \equiv \frac{\varphi}{cos\varphi + sin\varphi} \cdot (cos\varphi + sin\varphi)$. In general, the following asymptotic relations can be derived:

$$\varphi_{|sin\varphi| \to 0} \to \begin{cases} arcsin\varphi, & cos\varphi > 0 \\ \pi - arcsin\varphi, & cos\varphi < 0 \end{cases}, \tag{30}$$

$$\varphi_{|cos\varphi| \to 0} \to \begin{cases} arccos\varphi, & sin\varphi > 0 \\ -arccos\varphi, & sin\varphi < 0 \end{cases}, \tag{31}$$

$$\varphi_{|sin\varphi| \to |cos\varphi|} \to \frac{1}{2} \cdot (arc|sin\varphi| + arc|cos\varphi|) + k \cdot \frac{\pi}{2}, \tag{32}$$

where factor k depends on the signs of the functions $sin\varphi$ and $cos\varphi$ as shown in Tab.2.

Table 2 – The factor k values

k	0	1	–1	–2
Sign of $sin\varphi$	+1	–1	+1	–1
Sign of $cos\varphi$	+1	+1	–1	–1

Linear weighted phase detection determined in (29) – (32) enables high precision phase modulation of radiofrequency carrier signal in unlimited open interval $-\infty < \varphi_t < +\infty$ until function φ_t is continuous in time. The instant frequency ω_t of phase modulated harmonic carrier is determined by the instant derivative of phase: $\omega_t = \frac{\partial \varphi_t}{\partial t}$. In case of harmonic phase modulation function $\varphi_t = sin(\varpi \cdot t)$ we obtain instant frequency of modulated carrier: $\omega_t = \frac{\partial\, sin(\varpi \cdot t)}{\partial t} = \varpi \cdot cos(\varpi \cdot t)$. So, it is clear, that instant frequency ω_t of modulated signal will continuously oscillate around the equilibrium point (carrier frequency ω_0) in the range of $\omega_0 - \varpi \le \omega_t \le \omega_0 + \varpi$.

Thus, expected physical spectrum power distribution of harmonically modulated phase of the carrier is limited continuous function. However, commonly this signal is presented as a unlimited discrete Fourier series (consider formally modulated signal be periodic in time). This logical contradiction can be eliminated due the more accurate definition of how to evaluate the spectrum of non-periodic signal sample within the observation interval. To perform ODFM spectrum modulation the method of piecewise linear phase modulation can be applied [6], [9], [10].

Conclusion

One of the key issues in broadband radio access network design is comprehensive adaptation of transmission bit rate to the dynamically changed state of physical wireless link aimed to provide maximal channel performance along with appropriate minimization of bit error rate. The modern mobile communication technologies based on the LTE standard typically have three possible options for transmission bit rate control through dynamic overleap between conventional subcarrier modulation types QPSK, 16QAM and 64QAM.

The introduced in this paper tensor model of I/Q-phase modulation forms a theoretical background on flexible channel performance adaptation in OFDM radio access network due to the variation of phase modulation depth in a wide range along with any particularly specified data coding technique. Further investigations on this subject implies utilization of piecewise linear functions in phase modulation and data coding. This approach initiates advanced researches on future generations of mobile and wireless networks contributed by Odesa national telecommunication academy in Ukraine.

References

1. Leon W.Couch, Digital and analog communication systems (8 edition, 2013, 789 pp. Available at http://www.slideshare.net/ovalence/digital-analog-communication-systems-8th-edition.

2. Chang R.W. ”Synthesis of Band-Limited Orthogonal Signals for Multichannel Data Transmission”, Bell Syst. Tech. J., vol.45, pp. 1775-1796, Dec. 1966.

3. Salzberg B.R. “Performance of an efficient parallel data transmission system”, IEEE Trans. Commun. Technol., vol. COM-15, pp. 805-813, Dec. 1967.

4. LTE-A PHY Layer Overview & Femto Design Challenges. Available at https://www.youtube.com/watch?v=JyKJ4_CybiE.

5. The Verizon Wireless 4G LTE Network: Transforming Business with Next-Generation Technology." 4G LTE WHITE PAPER (n.d.): n. pag. Web. 23 June 2015.

6. Vorobiyenko P.P. ,Tikhonov V.I., Taher A. The LTE Technology Perspectives in Multimedia applications, «Цифрові технології»,№17, 2015 – с.7-15.

7. Korn G., Korn T. “Mathematical handbook for scientists and engineers” McGraw-Hill Book Co., N.Y., 1968, 1097 pp.

8. Fundamentals of Tensor Analysis. MCEN 5023/ASEN 5012 Chapter 2 Fall, 2006,-32 pp. – Available at http://www.colorado.edu/MCEN/MCEN5023/chap_02.pdf.

9. Тіхонов В. І. Метод кодування символів у когерентному оптичному каналі інтегрованої технології телекомунікацій / В. І. Тіхонов // Восточно-Европейский журнал передовых технологий . - 2013. - № 5(2). - С. 8-12. - Режим доступу: http://nbuv.gov.ua/j-pdf/Vejpte_2013_5(2)__3.pdf.

10. Tikhonov V.I., A.Taher. An adaptive phase modulation for OFDM based radio channel. Матеріали ІІ-ї Міжнародної науково-практичної конф. «Інформаційні технології та взаємодії», Київ, листопад 2015, с.171–172.

Литература

1. Leon W.Couch, Digital and analog communication systems (8 edition, 2013, 789 pp. Available at http://www.slideshare.net/ovalence/digital-analog-communication-systems-8th-edition.

2. Chang R.W. ”Synthesis of Band-Limited Orthogonal Signals for Multichannel Data Transmission”, Bell Syst. Tech. J., vol.45, pp. 1775-1796, Dec. 1966.

3. Salzberg B.R. “Performance of an efficient parallel data transmission system”, IEEE Trans. Commun. Technol., vol. COM-15, pp. 805-813, Dec. 1967.

4. LTE-A PHY Layer Overview & Femto Design Challenges. Available at https://www.youtube.com/watch?v=JyKJ4_CybiE.

5. The Verizon Wireless 4G LTE Network: Transforming Business with Next-Generation Technology." 4G LTE WHITE PAPER (n.d.): n. pag. Web. 23 June 2015.

6. Vorobiyenko P.P. ,Tikhonov V.I., Taher A. The LTE Technology Perspectives in Multimedia applications, «Цифрові технології»,№17, 2015 – с.7-15.

7. Korn G., Korn T. “Mathematical handbook for scientists and engineers” McGraw-Hill Book Co., N.Y., 1968, 1097 pp.

8. Fundamentals of Tensor Analysis. MCEN 5023/ASEN 5012 Chapter 2 Fall, 2006,-32 pp. – Available at http://www.colorado.edu/MCEN/MCEN5023/chap_02.pdf.

9. Тіхонов В. І. Метод кодування символів у когерентному оптичному каналі інтегрованої технології телекомунікацій / В. І. Тіхонов // Восточно-Европейский журнал передовых технологий . - 2013. - № 5(2). - С. 8-12. - Режим доступу: http://nbuv.gov.ua/j-pdf/Vejpte_2013_5(2)__3.pdf.

10. Tikhonov V.I., A.Taher. An adaptive phase modulation for OFDM based radio channel. Матеріали ІІ-ї Міжнародної науково-практичної конф. «Інформаційні технології та взаємодії», Київ, листопад 2015, с.171–172.

Рецензія/Peer review : 18.2.2016 р. Надрукована/Printed : 26.3.2016 р.